Geol. Mag. **156** (*6*), *2019, pp. 1105–1110* © *Cambridge University Press 2018*
doi:10.1017/S0016756818000481

RAPID COMMUNICATION

Mercury evidence from the Sino-Korean block for Emeishan volcanism during the Capitanian mass extinction

HYOSANG KWON, MUN GI KIM & YONG IL LEE*
School of Earth and Environmental Sciences, Seoul National University, Seoul 08826, Republic of Korea

(*Received* 12 September 2017; *accepted* 24 May 2018; *first published online* 28 August 2018)

Abstract

A prominent large negative $\delta^{13}C_{org}$ excursion and a coeval notable spike in mercury (Hg)/total organic carbon ratio are observed in the middle–upper Permian Gohan Formation in central Korea, located in the eastern Sino-Korean block (SKB), which may represent the Capitanian mass extinction event. The SKB was separated from the South China block by the eastern Palaeo-Tethys Ocean. This finding from the SKB supports the widespread Hg loading to the environment emitted from the Emeishan volcanic eruptions in SW China. This study demonstrates that the Hg cycle was globally perturbed in association with global carbon cycle perturbation that occurred during the Capitanian Extinction.

Keywords: Capitanian extinction, Emeishan volcanism, Gohan Formation, Sino-Korean block

1. Introduction

The Captanian mass extinction event had a major impact on the marine realm near the end of the middle Permian Period (Stanley & Yang, 1994; Bond *et al*. 2010*a*). The timing of the mass extinction has been in dispute; it is considered to be either the middle Capitanian (Shen & Shi, 2009; Bond *et al*. 2010*b*) or near the Capitanian–Wuchiapingian boundary (Kaiho *et al*. 2005; Groves & Wang, 2013; Day *et al*. 2015). This extinction event is generally characterized by a major negative carbon isotope excursion (Retallack *et al*. 2006; Bond *et al*. 2010*a*) and is known to have been associated with anoxia and acidification in the oceans; it was possibly caused by the volcanic eruptions that produced the Emeishan Traps in southwest China (Wignall *et al*. 2009; Bond *et al*. 2015).

In general, carbon isotopic compositions of terrestrial plants reflect carbon isotopes of CO_2 dissolved in ocean, as carbon as CO_2 is continuously exchanged between ocean and atmosphere. Extinction of many groups of marine organisms due to biotic crisis would have limited oceanic primary production, leading to less consumption of organic carbon and resulting in isotopically light dissolved CO_2 in the ocean. Enrichment of organic carbon (relatively enriched in ^{12}C) will result in a negative $\delta^{13}C$ excursion in the ocean–atmosphere system. As plants use carbon dioxide in the atmosphere through photosynthesis, this would result in a negative $\delta^{13}C$ excursion in plant matters in terrestrial environments. Many studies of continental organic matter have demonstrated that the atmospheric signal dominated over local factors such as taxonomic, environmental and diagenetic effects (Hasegawa, 1997; Gröcke, Hesselbo & Jenkyns, 1999; Arens, Jahren & Amundson, 2000; Hesselbo *et al*. 2007; Belcher *et al*. 2010; Nunn *et al*. 2010; Dal Corso *et al*. 2011).

A temporal link between continental flood basalt volcanism and mass extinction is well established (Courtillot & Renne, 2003; Wignall, 2005; Jourdan *et al*. 2014; Bond & Grasby, 2017; Ernst & Youbi, 2017), supporting the idea of a cause-and-effect relationship. This link between the Capitanian mass extinction event and eruption of Emeishan flood basalts has been demonstrated by Wignall *et al*. (2009). Investigation of the global influence of Emeishan volcanism is important for understanding the relationship between the mass extinction and the development of this igneous province. Volcanism is known to be a major natural source of mercury (Hg), emitting it as a trace gas (Pyle & Mather, 2003). A typical atmospheric residence time of gaseous elemental Hg is 0.5–2 years (Blum, Sherman & Johnson, 2014). Since Hg emitted from explosive volcanism is assumed to be transported long range in the atmosphere, it is globally distributed before being drawn down and eventually deposited in sediments. Sedimentary Hg is a proxy for volcanic volatiles, especially linked to large igneous provinces (LIPs), and has been reported in many recent studies (Sanei, Grasby & Beauchamp, 2012; Sial *et al*. 2013, 2014, 2016; Grasby *et al*. 2015, 2016; Percival *et al*. 2015, 2016, 2017; Font *et al*. 2016, 2018; Thibodeau & Bergquist, 2017). Grasby *et al*. (2016) reported an Hg anomaly associated with Capitanian extinction from Spitsbergen, Norway (NW Pangea), and suggested that the Hg loading to the environment may have been a contributing cause to the mass extinction event. More reports on Hg anomaly may strengthen the cause-and-effect scenario by supporting the close temporal link between the onset of large volcanic eruptions and extinction.

Here, we studied the volatile emissions and ocean–atmosphere impacts of the eruption of the Emeishan LIP in SW China by analysis of sedimentary mercury concentrations and carbon isotopic composition of organic matter in an upper Permian (Capitanian–Wuchiapingian) terrestrial sedimentary succession in the Taebaeksan Basin, central eastern Korea. During Permian time the Korean Peninsula belonged to the Sino-Korean block (SKB; also called the North China block). The SKB and the South China block were separated blocks within the eastern Palaeo-Tethys Ocean before their amalgamation during Triassic time (Meng & Zhang, 1999). The Taebaeksan Basin in the

*Author for correspondence: lee2602@plaza.snu.ac.kr

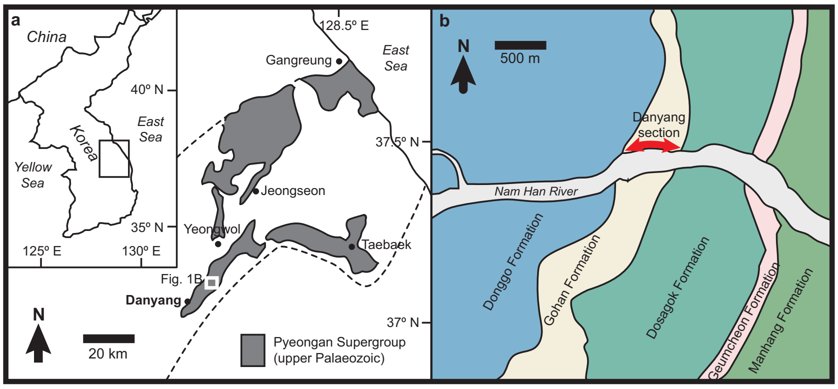

Figure 1. (Colour online) (a) The grey areas represent the coalfields with distribution areas of the Pyeongan Supergroup in central eastern Korea. The dotted lines represent the boundaries of the Taebaeksan Basin. (b) Geological map (after Park *et al*. 1975) showing the location of the Danyang section in the Danyang coalfield (white boxed area in (a)). The stratigraphic top is to the NW.

eastern SKB was situated at low palaeolatitudes (*c.* 6° N; Doh & Piper, 1994). This study reports a record in the SKB that there was a potential environmental impact due to volatile emissions from the Emeishan LIP and demonstrates that the Hg cycle was indeed perturbed on a global scale during the Capitanian extinction.

2. Geological setting

In South Korea, upper Palaeozoic sediments (the Pyeongan Supergroup) are distributed in several coalfields in the Taebaeksan Basin (Fig. 1). The detritus for the Pyeongan Supergroup was mostly derived from recycled orogens located to the east and SE of the Korean Peninsula (Yu, Lee & Boggs, 1997; Lee & Sheen, 1998; Kim, Lee & Choi, 2017). The Gohan Formation in this study is from the Danyang coalfield (Fig. 1). The Gohan Formation in this coalfield consists dominantly of black to dark-grey shale with medium-bedded dark-grey coarse sandstone and light-green medium sandstone. The thickness of the Gohan Formation in this coalfield reaches 450 m.

As the middle–upper Permian deposits of the SKB are represented by terrestrial sequences, regional correlation and age determination have been largely dependent on the fossil plant biostratigraphy despite its limitations. Chun (1985, 1987) identified fossil plants such as *Lobatannularia heianensis*, *Sphenophyllum* sp. cf. *kawasaki*, *Gigantopteris nicotianefolia*, *Alethopteris huiana*, *Compsopteris contracta*, *C. wongii*, *Cladophlebis* sp., *Taeniopteris multinervis*, *Chiropteris reniformis*, *Cordaites principalis*, *Pterophyllum diahoensis* and *Pt.* sp. cf. *nilssonioides* in the Gohan Formation, and established the *G. nicotianaefolia–Ch. reniformis–L. heianensis* Assemblage. Detailed investigation on the underlying stratigraphic unit, the Dosagok Formation, revealed that the base of this assemblage lies in the middle–upper part of the Dosagok Formation (S. Y. Kim, unpub. M.Sc. thesis, Seoul National University, 1985). Characterized by the occurrence of the *Gigantopteris* and several others including *L. heianensis*, its floral composition is largely similar to some known assemblages in North China which have been generally attributed to the Capitanian–Wuchiapingian (refer to Wang, 2010 for summary on the upper Palaeozoic fossil plant assemblages in North China). These assemblages also share the feature that they follow the demise of older plant species such as *Emplectopteris triangularis*. At the section near Taiyuan, Shanxi Province, Stevens *et al*. (2011) correlated the horizon of a similar floral change to the Roadian (Lower Shihhotse Formation or LSF extinction); such age correlation deviates widely from other studies conducted in North China however, probably due to an inaccurate assignment of the Illawara geomagnetic reversal horizon in their section. In the Taebaeksan Basin, it has been reported that the Dosagok Formation records both the normal and reversed geomagnetic polarities (Doh, 1995), and therefore the stratigraphic horizon of the Illawara reversal should be placed either within or below the Dosagok Formation. The information from both biostratigraphy and palaeomagnetism suggests that the Dosagok Formation has a Wordian–Capitanian depositional age. The exact depositional ages of the base and top of the Gohan Formation remain speculative. However, given that only the reversed geomagnetic polarity was reported from randomly collected samples of the Gohan Formation (Doh, 1995), the depositional age for much of this formation is likely to correspond to the Wuchiapingian Age, the time interval dominated by reversed polarity (Hounslow & Balabanov, 2016; Lucas & Shen, 2017). The mean youngest age of detrital zircons from the Gohan Formation sandstone is 261 ± 2.5 Ma (Lee, Choi & Orihashi, 2012), which further supports this interpretation. While the lower part of the Gohan Formation may correspond to the timing of the Capitanian extinction and/or the Emeishan volcanism, direct evidence of extinction has not been reported from this formation.

3. Methods

A total of 143 samples were collected with a sampling interval of 2.5 m at the Danyang section (Fig. 1b). Total organic carbon (TOC) content was analysed using a carbon-nitrogen (CN) elemental analyser (FlashEA 1112), and carbon isotopic values of organic matter ($\delta^{13}C_{org}$) were analysed by a stable isotope ratio mass spectrometer (IsoPrime-EA, Micromass, UK) interfaced with an elemental analyser at the National Instrumentation Center for Environmental Management, Seoul National University. Carbon isotopic values were presented in parts per thousand (‰) deviation from the Peedee Belemnite (PDB). The analytical precision based on repeated measurements of the laboratory standard was better than ±0.1 ‰ (i.e. Hong & Lee, 2013). Mercury concentration was analysed by a Milestone DMA-80 direct mercury analyser following standard methods (American Society for Testing and Materials, 2006) at Chungnam National University. Each sample was measured three times and the results were averaged. Trace element composition was analysed by a VG elemental PQII and an inductively coupled plasma mass spectrometer at the Korea Basic Science Institute.

https://doi.org/10.1017/S0016756818000481 Published online by Cambridge University Press

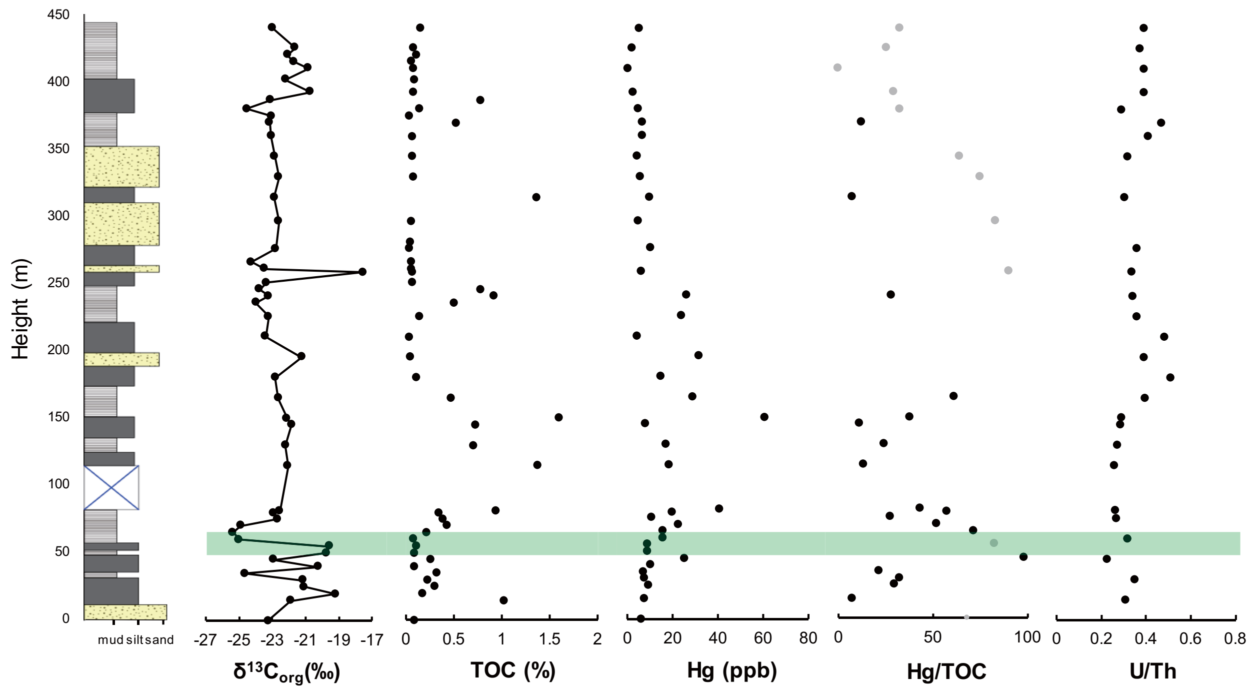

Figure 2. (Colour online) Plots of geochemical data from the Danyang section showing carbon isotope values for organic carbon, Hg values, Hg (ppb) normalized by TOC (%) (the Hg/TOC values are shown in black for values of TOC >0.2 % and grey for TOC values <0.2 %), percent total organic carbon (TOC) and U/Th ratios (ratios from sandstones are excluded). The horizontal bar represents the level of the interpreted Capitanian mass extinction event.

4. Results and discussion

The average background Hg value is 6 ppb. Hg values in the basal 40 m are 6–9 ppb and then show a shift at 45 m to a value of 25 ppb, followed by a subsequent decline to 8 ppb at 50–55 m. In the section interval from 60 m to 239 m level, Hg concentrations show an order of magnitude higher than the background value. In the remaining upper part of the section the Hg concentration is low, less than 10 ppb with an average of 5 ppb. The Hg concentrations are plotted in Figure 2.

As sedimentary drawdown of Hg is typically achieved via organic matter (Benoit *et al.* 2001; Outridge *et al.* 2007), sedimentary Hg concentrations are normalized against TOC to account for the effect on Hg drawdown by changes in organic matter deposition rates (Sanei, Grasby & Beauchamp, 2012). TOC content is generally less than 0.3 %, with some values reaching 1.6 %. Given the low organic matter content throughout much of the Danyang section, reliable Hg/TOC ratios are not always possible to obtain. For values of < 0.2 % TOC, inaccuracies in measurement can lead to magnified errors and highly variable Hg/TOC values that are not reflective of natural conditions (*cf.* Grasby *et al.* 2016). These data were marked in grey for consideration when interpreting Figure 2. For TOC values of > 0.2 %, broad spikes in both Hg concentrations as well as Hg/TOC values are noted in the 45–81 m section interval.

The $\delta^{13}C_{org}$ data from the Danyang section show initially relatively fluctuating values between –23.3 ‰ and –19.2 ‰ from the base to *c.* 60 m, at which a pronounced negative shift (5.8 ‰) occurs. The carbon/nitrogen (C/N) ratio of organic matter is less than 10, suggestive of lacustrine algae during the $\delta^{13}C_{org}$ negative excursion. However, given the low TOC content (< 0.5 %) in most samples, including the negative carbon excursion level, the possibility of artificially depressed C/N ratios cannot be excluded considering that the proportion of inorganic nitrogen can be relatively high in the residual nitrogen (Meyers & Teranes, 2001). Such a large negative carbon isotope excursion implies a major perturbation to the carbon cycle. After this point there is a progressive recovery through the next 10 m before the covered interval to –23 ‰, the general background value. A weak positive excursion (–21.2 ‰) occurs at the 194 m level, followed by a strong positive excursion to –17.6 ‰ at 256 m. At the top of the Danyang section two weak positive peaks (–20.7 ‰ and –20.8 ‰) are noted.

As clay minerals are the alternative host for scavenging Hg in sediment via adsorption and subsequent deposition (Kongchum, Hudnall & Delaune, 2011), we also analysed Al_2O_3 content of the studied samples. Correlation between Al_2O_3 content and Hg concentration ($R = –0.08$, $p = 0.66$) is lacking, indicating that Hg fluctuations are not controlled primarily by clay content. Because Hg is sensitive to anoxia and heating, it may undergo transformations and possible migration, resulting in losses of Hg (Bergquist, 2017). However, the measured redox-sensitive elemental ratios (U/Th) are less than 0.6 in the Danyang section, which suggests that the water column in the depositional environment was under oxygenated conditions (*cf.* Jones & Manning, 1994) and the elevated Hg/TOC spike level does not show changes in redox state, suggestive of the elevated Hg/TOC ratios resulting from Hg input. The facies changes that might have affected the Hg shift were not observed in thin-sections (online Supplementary Fig. S1, available at http://journals.cambridge.org/geo).

In the lower part of the Danyang section an abrupt increase in Hg concentrations and Hg/TOC ratios are correlated with the negative excursion in $\delta^{13}C_{org}$. As the Capitanian extinction event is characterized by the globally observed $\delta^{13}C$ negative excursion (Bond *et al.* 2015; Grasby *et al.* 2015), occurring coevally with Hg anomaly (Grasby *et al.* 2016), the correlation between Hg/TOC excursion and

https://doi.org/10.1017/S0016756818000481 Published online by Cambridge University Press

negative $\delta^{13}C_{org}$ excursion is tentatively suggestive of a perturbation to the global Hg and carbon cycles at the extinction event. While it is difficult to provide a comprehensive age model, this correlation allows the Hg/TOC increase to be stratigraphically matched to the Emeishan LIP volcanism. Accordingly, the stratigraphic level showing both the negative excursion in $\delta^{13}C_{org}$ and Hg/TOC spikes may mark the Capitanian extinction event recorded in the Gohan Formation.

5. Conclusions

A prominent negative $\delta^{13}C_{org}$ excursion occurs in the lower Gohan Formation in Danyang, central eastern Korea. A mercury anomaly is also observed in the lower part of the Danyang section. The mercury anomaly occurs at the same level with a prominent negative $\delta^{13}C_{org}$ excursion. The coincidence of timing between the negative $\delta^{13}C_{org}$ excursion and mercury anomaly strongly suggests that this level may represent the record of the Capitanian mass extinction event in the Gohan Formation. This case study from the SKB, separated from the South China block with the Emeishan LIP, demonstrates that the Hg cycle was globally perturbed in association with the global carbon cycle perturbation that occurred during the Capitanian mass extinction.

Acknowledgements. This work was supported by the National Research Foundation of Korea (grant no. 2014R1A2A2A01005404). We thank the journal editor, Professor S.M. Hubbard, and two anonymous journal reviewers for their constructive comments which led to the improvement of our manuscript.

Supplementary material

To view supplementary material for this article, please visit https://doi.org/10.1017/S0016756818000481

References

American Society for Testing and Materials. 2006. Standard test method for total mercury in coal and coal combustion residues by direct combustion analysis: ASTM D6722-01. West Conshohocken, Pennsylvania, ASTM International, 4 p.

Arens, N. C., Jahren, A. H. & Amundson, R. 2000. Can C3 plants faithfully record the carbon isotopic composition of atmospheric carbon dioxide? *Paleobiology* **26**, 137–64.

Belcher, C. M., Mander, L., Rein, G., Jervis, F. X., Haworth, M., Hesselbo, S. P., Glasspool, I. J. & McElwain, J. C. 2010. Increased fire activity at the Triassic/Jurassic boundary in Greenland due to climate-driven floral change. *Nature Geoscience* **3**, 426–9.

Benoit, J. M., Mason, R. P., Gilmour, C. C. & Aiken, G R. 2001. Constraints for mercury binding by dissolved organic matter isolates from the Florida Everglades. *Geochimica et Cosmochimica Acta* **65**, 4445–51.

Bergquist, B. A. 2017. Mercury, volcanism, and mass extinctions. *Proceedings of National Academy of Sciences* **114**, 8675–7.

Blum, J. D., Sherman, L. S. & Johnson, M. W. 2014. Mercury isotopes in earth and environmental sciences. *Annual Review of Earth and Planetary Sciences* **42**, 249–69.

Bond, D. P. & Grasby, S. E. 2017. On the causes of mass extinctions. *Palaeogeography, Palaeoclimatology, Palaeoecology* **478**, 3–29.

Bond, D. P. G., Hilton, J., Wignall, P. B., Ali, J. R., Stevebs, L. G., Sun, Y. & Lai, X. 2010a. The Middle Permian (Capitanian) mass extinction on land and in the oceans. *Earth-Science Reviews* **102**, 100–16.

Bond, D. P. G., Wignall, P. B., Joachimski, M. M., Sun, Y., Savov, I., Grasby, S. E., Beauchamp, B. & Blomeier, D. P. G. 2015. An abrupt extinction in the Middle Permian (Capitanian) of the boreal realm (Spitsbergen) and its link to anoxia and acidification. *Geological Society of America Bulletin* **127**, 1411–21.

Bond, D. P. G., Wignall, P. B., Wang, W., Izon, G., Jiang, H.-S., Lai, X.-L., Sun, Y.-D., Newton, R. J., Shao, L.-Y., Védrine, S. & Cope, H. 2010b. The mid-Capitanian (Middle Permian) mass extinction and carbon isotope record of South China. *Palaeogeography, Palaeoclimatology, Palaeoecology* **292**, 282–94.

Chun, H. Y. 1985. Permo-Carboniferous plant fossils from the Samcheog coalfield, Gangweondo, Korea. Part 1. *Journal of Paleontological Society of Korea* **1**, 95–122.

Chun, H. Y. 1987. Permo-Carboniferous plant fossils from the Samcheog coalfield, Gangweondo, Korea. Part 2. *Journal of Paleontological Society of Korea* **3**, 1–27.

Courtillot, V. E. & Renne, P. R. 2003. On the ages of flood basalt events. *Comptes Rendus Geoscience* **335**, 113–40.

Dal Corso, J., Preto, N., Kustatscher, E., Mietto, P., Roghi, G. & Jenkyns, H. C. 2011. Carbon-isotope variability of Triassic amber, as compared with wood and leaves (Southern Alps, Italy). *Palaeogeography, Palaeoclimatology, Palaeoecology* **302**, 187–93.

Day, M. O., Ramezani, J., Bowring, S. A., Sadler, P. M., Erwin, D. H., Abdala, F. & Rubidge, B. S. 2015. When and how did the terrestrial mid-Permian mass extinction occur? Evidence from the tetrapod record of the Karoo Basin, South Africa. *Proceedings of the Royal Society B* **282**: 20150384.

Doh, S.-J. 1995. Paleomagnetism of the Pyeongan Supergroup in the Samcheok area. *Economic and Environmental Geology* **28**, 559–69 (in Korean with English abstract).

Doh, S.-J. & Piper, J. D. A. 1994. Palaeomagnetism of the (Upper Palaeozoic–Lower Mesozoic) Pyongan Supergroup, Korea: a Phanerozoic Link with the North China Block. *Geophysical Journal International* **117**, 850–63.

Ernst, R. E. & Youbi, N. 2017. How Large Igneous Provinces affect global climate, sometimes cause mass extinctions, and represent natural markers in the geological record. *Palaeogeography, Palaeoclimatology, Palaeoecology* **478**, 30–52.

Font, E., Adatte, T., Andrade, M., Keller, G., Bitchong, A. M., Carvallo, C., Ferreira, J., Diogo, Z. & Mirão, J. 2018. Deccan volcanism induced high-stress environment during the Cretaceous–Paleogene transition at Zumaia, Spain: Evidence from magnetic, mineralogical and biostratigraphic records. *Earth and Planetary Science Letters* **484**, 53–66.

Font, E., Adatte, T., Sial, A. N., Drude de Lacerda, L., Keller, G. & Punekar, J. 2016. Mercury anomaly, Deccan volcanism, and the end-Cretaceous mass extinction. *Geology* **44**, 171–4.

Grasby, S. E., Beauchamp, B., Bond, D. P. G. & Wignall, P. B. 2016. Mercury anomalies associated with three extinction events (Capitanian Crisis, Latest Permian Extinction and the Smithian/Spathian Extinction) in NW Pangea. *Geological Magazine* **153**, 285–97.

GRASBY, S. E., BEAUCHAMP, B., BOND, D. P. G., WIGNALL, P. B., TALAVERA, C., GALLOWAY, J. M., PIEPJOHN, K., REINHARDT, L. & BLOMEIER, D. 2015. Progressive environmental deterioration in NW Pangea leading to the Latest Permian Extinction. *Geological Society of America Bulletin* **127**, 1331–47.

GRÖCKE, D. R., HESSELBO, S. P. & JENKYNS, H. C. 1999. Carbon-isotope composition of Lower Cretaceous fossil wood: Ocean–atmosphere chemistry and relation to sea-level change. *Geology* **27**, 155–8.

GROVES, J. R. & WANG, Y. 2013. Timing and size selectivity of the Guadalupian (Middle Permian) fusulinoidean extinction. *Journal of Paleontology* **87**, 183–96.

HASEGAWA, T. 1997. Cenomanian–Turonian carbon isotope events recorded in terrestrial organic matter from northern Japan. *Palaeogeography, Palaeoclimatology, Palaeoecology* **130**, 251–73.

HESSELBO, S. P., JENKYNS, H. C., DUARTE, L. V. & OLIVEIRA, L. C. V. 2007. Carbon-isotope record of the Early Jurassic (Torcian) Oceanic Anoxic Event from fossil wood and marine carbonate (Lusitanian Basin, Portugal). *Earth and Planetary Science Letters* **253**, 455–70.

HONG, S. K. & LEE, Y. I. 2013. Contributions of soot to $\delta^{13}C$ of organic matter in Cretaceous lacustrine deposits, Gyeongsang Basin, Korea: implication for paleoenvironmental reconstructions. *Palaeogeography, Palaeoclimatology, Palaeoecology* **371**, 54–61.

HOUNSLOW, M. W. & BALABANOV, Y. P. 2016. A geomagnetic polarity timescale for the Permian, calibrated to stage boundaries. In *The Permian Timescale* (eds S. G. Lucas & S. Z. Chen), pp. 61–103. Geological Society of London, Special Publication no. 450.

JONES, B. & MANNING, D. A. C. 1994. Comparison of geochemical indices used for the interpretation of palaeoredox conditions in ancient mudstones. *Chemical Geology* **111**, 111–29.

JOURDAN, F., HODGES, K., SELL, B., SCHALTEGGER, U., WINGGATE, M. T. D., EVINS, L. Z., SÖDERLUND, U., HAINES, P. W., PHILLIPS, D. & BLENKINSOP, T. 2014. High-precision dating of the Kalkarindji large igneous province, Australia, and synchrony with the Early–Middle Cambrian (Stage 4–5) extinction. *Geology* **42**, 543–6.

KAIHO, K., CHEN, Z. Q., OHASHI, T., ARINOBU, T., SAWADA, K. & CRAMER, B. S. 2005. A negative carbon isotope anomaly associated with the earliest Lopingian (Late Permian) mass extinction. *Palaeogeography, Palaeoclimatology, Palaeoecology* **223**, 172–80.

KIM, M., LEE, Y. I. & CHOI, T. 2017. The tectonic setting of the eastern margin of the Sino-Korean Block inferred from detrital zircon U–Pb age and Nd isotope composition of the Pyeongan Supergroup (late Paleozoic–Early Triassic), Korea. *Geological Magazine*, published online 20 November 2017, doi: 10.1017/S0016756817000899.

KONGCHUM, M., HUDNALL, W. H. & DELAUNE, R. D. 2011. Relationship between sediment clay minerals and total mercury. *Journal of Environmental Science and Health, Part A* **46**, 534–9.

LEE, Y. I., CHOI, T. & ORIHASHI, Y. 2012. Depositional ages of upper Pyeongan Supergroup strata in the Samcheok coalfield, eastern central Korea. *Journal of Geological Society of Korea* **48**, 93–9 (in Korean).

LEE, Y. I. & SHEEN, D.-H. 1998. Detrital modes of the Pyeongan Supergroup (Late Carboniferous–Early Triassic) sandstones in the Samcheog coalfield, Korea: implications for provenance and tectonic setting. *Sedimentary Geology* **119**, 219–38.

LUCAS, S. G. & SHEN, S. Z. 2017. The Permian timescale: an introduction. In *The Permian Timescale* (eds S. G. Lucas & S. Z. Chen), pp. 1–19. Geological Society of London, Special Publication no. 450.

MENG, Q.-R. & ZHANG, G.-W. 1999. Timing of collision of the North and South China blocks: Controversy and reconciliation. *Geology* **27**, 123–6.

MEYERS, P. A. & TERANES, J. L. 2001. Sediment organic matter. In *Tracking Environmental Change Using Lake Sediments. Volume* **2***: Physical and Geochemical Methods* (eds W.M. Last & J.P. Smol), pp. 239–69. New York: Springer.

NUNN, E. V., PRICE, G. D., GRÖCKE, D. R., BARABOSHKIN, E. Y., LENG, M. J. & HART, M. B. 2010. The Valanginian positive carbon isotope event in Arctic Russia: Evidence from terrestrial and marine isotope records and implications for global carbon cycling. *Cretaceous Research* **31**, 577–92.

OUTRIDGE, P. M., SANEI, L. H., STERN, G. A., HAMILTON, P. B. & GOODARZI, F. 2007. Evidence for control of mercury accumulation rates in Canadian High Arctic lake sediments by variations of aquatic primary productivity. *Environmental Science Technology* **41**, 5259–65.

PARK, J. S., SHIN, M. S., JEONG, C. S., LEE, M. H., YOON, Y.D., KIM, S. H. & HWANG, H. S. 1975. Geological investigation report of Danyang coal field. Korea Institute of Geoscience and Mineral Resources, 54 pp (in Korean with English abstract).

PERCIVAL, L. M. E., COHEN, A. S., DAVIES, M. K., DICKSON, A. J., HESSELBO, S. P., JENKYNS, H. C., LENG, M. J., MATHER, T. A., STORM, M. S. & XU, W. 2016. Osmium-isotope evidence for two pulses of increased continental weathering linked to volcanism and climate change during the Early Jurassic. *Geology* **44**, 759–62.

PERCIVAL, L. M. E., RUHL, M., HESSELBO, S. P., JENKYNS, H. C. & MATHER, T. A. 2017. Mercury evidence for pulsed volcanism during the end-Triassic mass extinction. *Proceedings of National Academy of Sciences of the USA* **114**, 7929–34.

PERCIVAL, L. M. E., WITT, M. L. I., MATHER, T. A., HERMOSO, M., JENKYNS, H. C., HESSELBO, S. P., AL-SUWAIDI, A. H., STORM, M. S., XU, W. & RUHL, M. 2015. Globally enhanced mercury deposition during the end-Pliensbachian and Toarcian OAE: A link to the Karoo-Ferrar large Igneous Province. *Earth and Planetary Science Letters* **428**, 267–80.

PYLE, D. M. & MATHER, T. A. 2003. The importance of volcanic emissions in the global atmospheric mercury cycle. *Atmospheric Environment* **37**, 5115–24.

RETALLACK, G. J., METZGER, C. A., GREAVER, T., JAHREN, A. H., SMITH, R. M. & SHELDON, N. D. 2006. Middle-Late Permian mass extinction on land. *Geological Society of America Bulletin* **118**, 1398–411.

SANEI, H., GRASBY, S. E. & BEAUCHAMP, B. 2012. Latest Permian mercury anomalies. *Geology* **40**, 63–6.

SHEN, S. Z. & SHI, G. R. 2009. Latest Guadalupian brachiopods from the Guadalupian/Lopingian boundary GSSP section at Penglaitan in Laibin, Guangxi, South China and implications for the timing of the pre-Lopingian crisis. *Palaeoworld* **18**, 152–61.

SIAL, A. N., CHEN, J., LACERDA, L. D., FREI, R., TEWARI, V. C., PANDIT, M. K., GAUCHER, C., FERREIRA, V. P., CIRILLI, S., PERALTA, S., KORTE, C., BARBOSA, J. A. & PEREIRA, N. S. 2016. Mercury enrichment and Hg isotopes in Cretaceous–Paleogene boundary successions: Links to volcanism and palaeoenvironmental impacts. *Cretaceous Research* **66**, 60–81.

https://doi.org/10.1017/S0016756818000481 Published online by Cambridge University Press

SIAL, A. N., CHEN, J., LACERDA, L. D., PERALTA, S., GAUCHER, C., FREI, R., CIRILLI, S., FERREIRA, V. P., MARQUILLAS, R. A., BARBOSA, J. A., PEREIRA, N. S. & BELMINO, I. K. C. 2014. High-resolution Hg chemostratigraphy: A contribution to the distinction of chemical fingerprints of the Deccan volcanism and Cretaceous–Paleogene Boundary impact event. *Palaeogeography, Palaeoclimatology, Palaeoecology* **414**, 98–115.

SIAL, A. N., LACERDA, L. D., FERREIRA, V. P., FREI, R., MARQUILLAS, R. A., BARBOSA, J. A., GAUCHER, C., WINDMÖLLER, C. C. & PEREIRA, N. S. 2013. Mercury as a proxy for volcanic activity during extreme environmental turnover: The Cretaceous–Paleogene transition. *Palaeogeography, Palaeoclimatology, Palaeoecology* **387**, 153–64.

STANLEY, S. M. & YANG, X. 1994. A double mass extinction at the end of the Paleozoic Era. *Science* **266**, 1340–44.

STEVENS, L. G., HILTON, J., BOND, D. P. G., GLASSPOOL, I. J. & JARDINE, P. E. 2011. Radiation and extinction patterns in Permian floras from North China as indicators for environmental and climate change. *Journal of the Geological Society* **168**, 607–19.

THIBODEAU, A. M. & BERGQUIST, B. A. 2017. Do mercury isotopes record the signature of massive volcanism in marine sedimentary records? *Geology* **45**, 95–6.

WANG, J. 2010. Late Paleozoic macrofloral assemblages from Weibei Coalfield, with reference to vegetational change through the Late Paleozoic Ice-age in the North China Block. *International Journal of Coal Geology* **83**, 292–317.

WIGNALL, P. 2005. The link between large igneous province eruptions and mass extinction. *Elements* **1**, 293–7.

WIGNALL, P., SUN, Y., BOND, D. P. G., IZON, G., NEWTON, R. J., VÉDRINE, S., WIDDOWSON, M., ALI, J. R., LAI, X., JIANG, H., COPE, H. & BOTTRELL, S. H. 2009. Volcanism, mass extinction, and carbon isotope fluctuations in the Middle Permian of China. *Science* **324**, 1179–82.

YU, K.-M., LEE, G.-H. & BOGGS, S. 1997. Petrology of late Paleozoic-early Mesozoic Pyeongan Group sandstones, Gohan area, South Korea and its provenance and tectonic implications. *Sedimentary Geology* **109**, 321–38.